Effect of NTC Behavior on the Characteristic Length Scale of Direct Detonation Initiation

Minh Bau Luong, Hong G. Im
Clean Combustion Research Center
King Abdullah University of Science and Technology, Thuwal 23955-6900, Saudi Arabia

Abstract

Direct detonation initiation (DDI) emerging from a hot spot requires a minimum runup distance to ensure the coherent coupling between the pressure wave and the heat release in the ignition zone. According to Zeldovich's theory, an ignition front is formed by a monotonic ignition delay distribution. Therefore, in principle, the characteristic length scale representing a runup distance of DDI should be based on the distribution of τ_{ig} over which τ_{ig} variation is monotonic. However, l_{hs} based on either temperature or concentration inhomogeneities is usually used. Thus, we proposed a new rigorous method to determine the *effective* runup distance l_{rd} of DDI regardless of the existence of the spatial variation of temperature or concentration inhomogeneous fields and the nonmonotonic ignition behavior due to the negative temperature coefficient (NTC) behavior. Particularly, l_{rd} is directly determined through the mean distance of dissipation elements of the 0D ignition delay field distribution, rather than relying solely on the temperature/concentration field. We found that the runup distance was shortened by approximately a factor of two for a hot spot that has temperature variation spanning across the NTC regime. As such, a longer hot-spot size is required for DDI. In addition, a better prediction of ignition modes was achieved by defining the normalized front speed as a statistical mean over each runup-distance element.

1 Introduction

Zeldovich [1] theory classified ignition regimes that rely on the speed of a spontaneous ignition front, S_{sp}, relative to the speed of a deflagration, S_L, and the speed of sound, a. S_{sp} is determined through the spatial gradient of the ignition delay time, $S_{sp} = |\nabla \tau_{ig}|^{-1}$. Based on this theory, Bradley and Gu [2, 3] further developed a $\xi - \varepsilon$ diagram to discen the ignition regimes where $\xi = a/S_{sp}$, and $\varepsilon = l_{hs}/(a\tau_e)$; ε is defined as the ratio of the residence time, l_{hs}/a, of the acoustic wave within the hot spot with a length of, l_{hs}, to the excitation time, τ_e.

This diagram has been widely used to identify the ignition modes of the end gas under highly-boosted engine conditions. For fuels that exhibit low-temperature chemistry (LTC), however, the prediction of ignition modes evolving from autoignitive hot spots becomes more complicated. Therefore, many studies have studied the effects of LTC and the associated negative temperature coefficient (NTC) regime on

Correspondence to: minhbau.luong@kaust.edu.sa (M.B. Luong)

the detonation peninsula [4–19]. It was found that a hot spot may induce multiple ignition fronts due to the low- and intermediate-temperature chemistry, and the interaction of multiple ignition fronts promotes detonation occurrence [7, 9, 11, 12]. Previous studies found that the prediction of ignition modes becomes inconsistent for different fuels in the presence of temperature/concentration inhomogeneities, especially for the fuels exhibiting a strong NTC behavior such as Dimethyl ether (DME) and *n*-heptane [7, 9, 11, 12].

The present study, therefore, proposes a new method to accurately determine the characteristic length scale of direct detonation initiation by autoignitive hot spots, so-called the *effective* runup distance l_{rd}, regardless of the existence of the nonmonotonic ignition behavior due to the negative temperature coefficient (NTC) behavior, and the spatial variation of temperature or concentration inhomogeneous fields [20–22]. In the presence of the NTC regime, the mean distance of dissipation elements of the ignition delay field, $\bar{l}_{DE}$, serves as the characteristic length scale of hot spots. The evaluation of $\xi - \varepsilon$ through l_{rd} allows a better prediction of ignition modes [11, 12].

2 Results and discussion

As shown in Fig. 1, Dimethyl ether (DME) exhibiting pronounced low-temperature chemistry with multi-stage ignitions and a strong negative temperature coefficient (NTC) behavior is chosen to represent NTC fuels. A 39-species skeletal mechanism [23] is used. The mechanism was validated over a wide range of engine conditions.

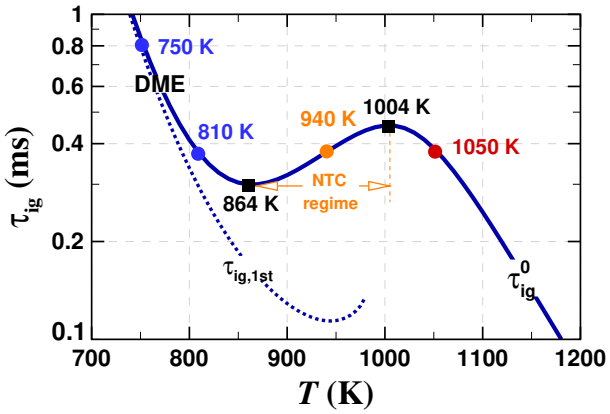

Fig. 1: Homogeneous ignition delay time of a stoichimometric DME/air mixture at constant volume of 40 atm as a function of temperature. $\tau_{ig,1}$ and τ^0_{ig} denotes the timing of the peak HRR of the first-stage ignition and the main ignition, respectively.

2.1 Analysis of one-dimensional hot spots

To reveal the effect of the NTC regime on the determination of l_{rd}, three distinct cases with varied T_{hs} are shown in Fig. 2In principle, the development of a detonation wave emerging from a hot spot, needs a minimum runup distance to ensure the mutual coupling between the pressure wave and the heat release in the ignition region. However, l_{hs} based on either temperature or concentration inhomogeneities that induce the τ_{ig} variation does not serve as an accurately representative quantity for the determination of l_{rd}, leading to an inaccurate evaluation of $\xi - \varepsilon$ [11, 12]. For example, when the range of temperature

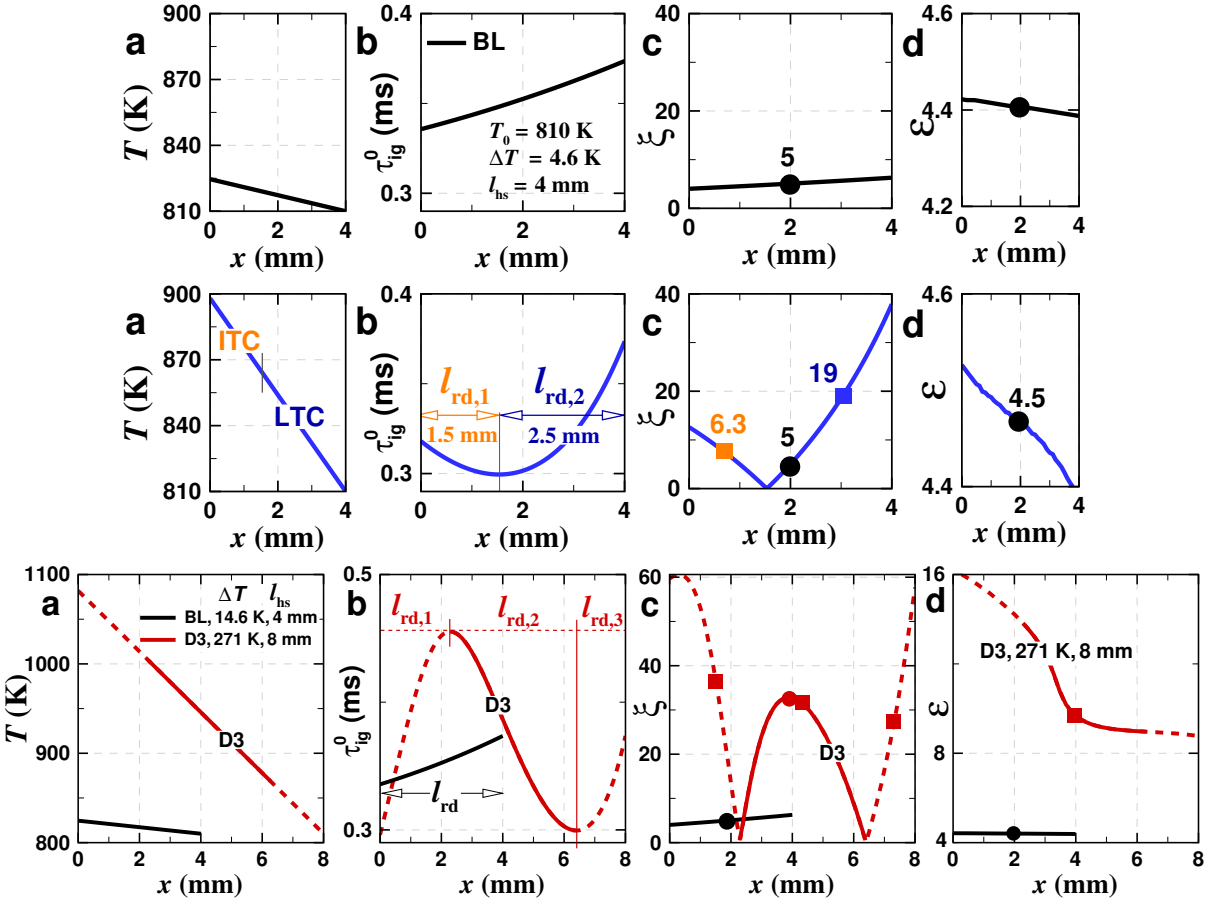

Fig. 2: **a** Initial temperature profile with T_0 of 810 K and varied T_{hs}, and **b-d** the spatial distribution of their corresponding τ_{ig}, ξ, ε. Dot symbols denote the midpoint of hot spots at which ξ and ε are computed. Square symbols indicate the mean $\bar{\xi}$ values. $l_{rd,1-3}$ denotes the τ_{ig}-based runup distance. BL and D denote baseline and detonation, respectively. **First row**: Baseline case with $T_0 = 810$ K and $\Delta T = 14.6$ K, resulting in $\xi = 5$ and $\varepsilon = 4.4$. **Second row**: 1D hot spot with $T_0 = 810$ K and $\Delta T = 88$ K, resulting in $\xi = 5$ and $\varepsilon = 4.5$ computed the midpoint of the hot spot (dot symbols), and the mean $\bar{\xi}_{1-2}$ values of 6.3 and 19. **Third row**: a 1D hot spot of Case D3 with $T_0 = 810$ K and $\Delta T = 271$ K resulting in three $l_{rd,1-3}$. The BL case also added for a direct comparison between D3 and BL [11].

variation crosses over the NTC regime, the *conventional* determination of ξ-ε by the midpoint of l_{hs} can lead to an inaccurate determination of ignition modes due to the non-monotonic τ_{ig} distribution.

As shown in Fig. 2, when the temperature variation spans across the NTC regime, τ_{ig} exhibits a non-monotonic distribution, leading to a decrease in l_{rd}. As such, it requires a longer l_{hs} to form DDI. The second row of Fig. 2 shows that when a hot spot has temperature lying in both low- and intermediate-temperature regimes, it induces a non-monotonic variation in τ_{ig} distribution. Particularly, the hot spot length of 4 mm is subdivided into two $l_{rd,1-2}$ elements of 1.5 mm, and 2.5 mm with the corresponding mean value of ξ of 6.3 and 19 computed for each l_{rd} element [11]. If computed at the midpoint of the hot spot, its $\xi = 5$ and $\varepsilon = 4.5$, meaning that DDI is expected for this case. However, unlike the BL case with $l_{rd} = l_{hs} = 4$ mm $> l_m$ that can form DDI, no DDI is observed for this case despite their $\xi = 5$ and $l_{hs} = 4$ mm. No DDI was found for this case [11] because the effective actual runup distance, $l_{rd,1-2}$, is approximately equal to a half of l_{hs} – insufficient runup distance to form DDI. If l_{rd} is used to compute ε, $\varepsilon = l_{rd}/a\tau_e$, no DDI is predicted to occur by this correction.

For Case D3 in the third row of Fig. 2, D3 with the increased l_{hs} of 8 mm can form DDI inside the hot spot. D3 With the large temperature variation spanning across the low-to-high temperature regime can develop into triple ignition fronts as dictated by three l_{rd} elements, l_{rd1}, l_{rd2}, and l_{rd3} that are associated with high-, intermediate-, and low-temperature chemistry, respectively (see [11]). Note that only the element associated with $l_{rd2} = 4.1$ mm can form DDI due to its sufficient runup distance, $l_{rd2} > l_m$ while the l_{rd1} and l_{rd3} elements cannot form DDI within their l_{rd} due to their much shorter l_{rd} and higher mean $\bar{\xi}$.

In summary, the low-temperature chemistry makes a prediction of ignition modes more complicated, especially if the temperature variation spans over the NTC regime. The length scale of the monotonic distribution of τ_{ig} is demonstrated to be more accurate in the interpretation of ignition modes. As such, ε_t and ξ determined at the midpoint of each l_{rd} element, and the mean value of ξ evaluated for each l_{rd} element should be adapted for a better prediction of ignition modes.

2.2 Statistical analysis of dissipation elements

From the understanding of the effect of the NTC regime on the determination of l_{rd} in the preceding 1D section, in the presence of the NTC regime, the τ_{ig}-based $\bar{l}_{DE}$ is found to be shorter than the temperature-based $\bar{l}_{DE}$ by approximately a factor of two [11, 12].In the multi-dimensional problems, consistently, the τ_{ig}-based $\bar{l}_{DE}$ should also be adopted in the computation of the predictive ξ_p and ε_p parameters [12].

According to the theory of dissipation elements [24], the characteristic length scale representing the size of hot spots in the isotropic temperature field fluctuations can be evaluated through the mean distance of dissipation elements (DE), $\bar{l}_{DE}$. Initially, l_{DE} is defined as the length scale over which the temperature profile is monotonic [24]. In the presence of the NTC regime, however, the τ_{ig} field is not monotonically varied with temperature. The τ_{ig}-based $\bar{l}_{DE}$ (the distance over which the τ_{ig} profile is monotonic, ranging from the peak to the trough of each dissipation element) is therefore carried out in this section in determining the characteristic length scale of hot spots instead of the temperature-based $\bar{l}_{DE}$ [12].

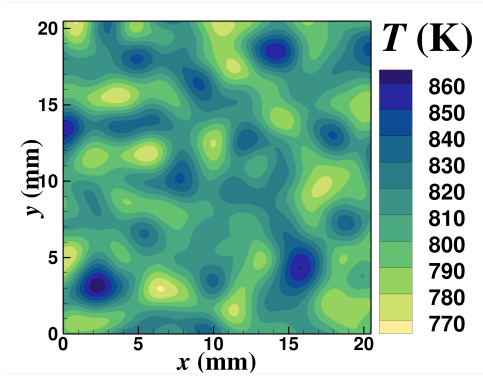

Fig. 3: Representative initial temperature field at T_0 of 810 K and T' of 15 K.

To quantitatively determine the characteristic length scale of hot spotsin the presence of the isotropic temperature field fluctuations as representatively shown in Fig. 3, the initial field of τ_{ig} is decomposed into *dissipation elements* (DE) instead of decomposing the initial temperature field. DE of τ_{ig} of two contrasting cases (T_0 of 810 K versus 864 K) together with their probability density function (PDF) at various T_0 and $T' = 15$ K are shown Fig. 4 and Fig. 5. As readily seen in Fig. 4 and Fig. 5, T_0 of 864 K (one of the extrema of τ_{ig} in the NTC regime in Fig. 1) exhibits a narrower range of l_{DE} distribution and thus a smaller mean $\bar{l}_{DE}$ than that of T_0 outside the NTC regime. $\bar{l}_{DE}$ as a function of T_0 in Fig. 6

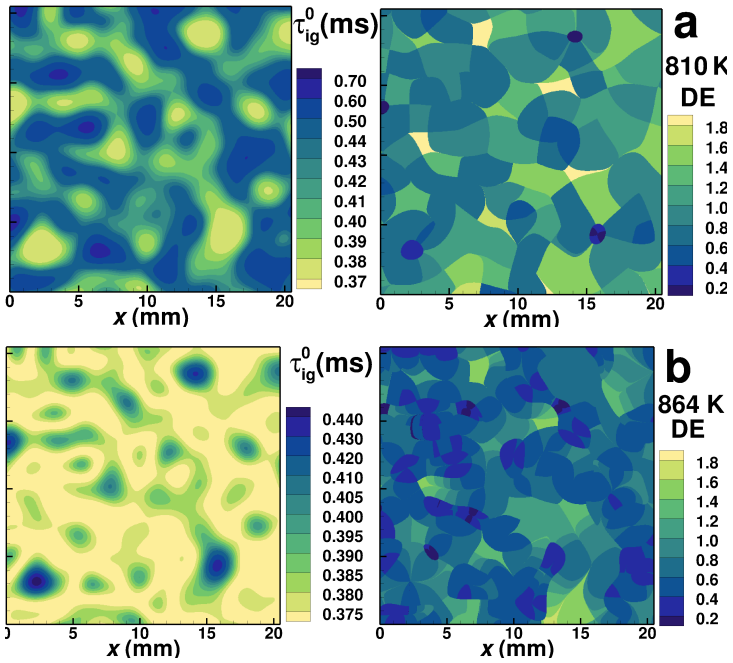

Fig. 4: Spatial distributions of τ_{ig} and dissipation elements (DE) at T_0 of **a** 810 K and **b** 864 K and $T' = 15$ K.

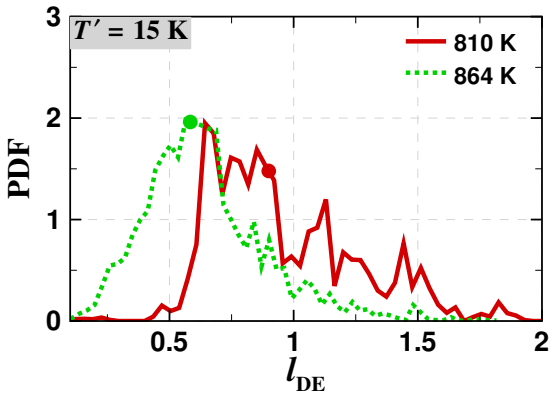

Fig. 5: PDF of dissipation elements (DE) at different T_0 and T' of 15 K. Dots denote the mean value of DE, $\bar{l}_{DE}$.

reveals that $\bar{l}_{DE}$ of T_0 in the vicinity of the extrema of the NTC regime becomes smaller almost by a half. Three l_T values are analyzed in Fig. 6 to show a consistently observed trend.

Unlike the τ_{ig}-based $\bar{l}_{DE}$, $\bar{l}_{DE}$ of the baseline (BL), which is obtained by decomposing the temperature field into DE, does not show the shortened $\bar{l}_{DE}$ in this regime, indicating that the temperature-based $\bar{l}_{DE}$ may lead to an inaccurate determination of the characteristic length scale of hot spots for NTC fuels. For the isotropic energy spectrum adopted in this study, we found that $\bar{l}_{DE}$ is approximately equal to a half of the two-point autocorrelation integral length scale, $\bar{l}_{DE} \cong l_{et}/2$ for non-NTC fuels.

We are performing multi-dimensional direct numerical simulations (DNS) over a wider spectrum of different initial conditions under internal combustion (IC) engine conditions for a comprehensive validation of the predictive accuracy of our proposed model [12]. More detailed information will be discussed in

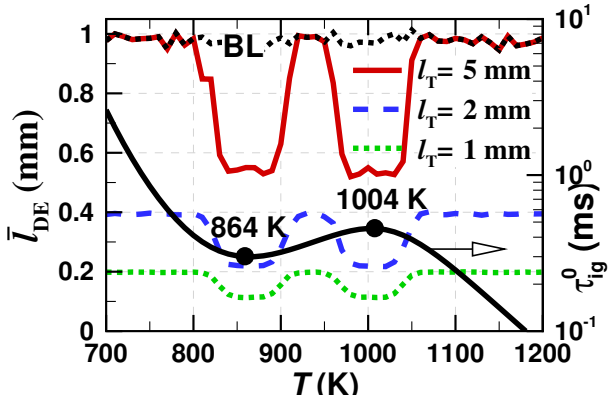

Fig. 6: The mean distance of dissipation elements (DE) against T_0 at three l_T and T' of 15 K. Two dots mark the extrema of τ_{ig}.

the presentation.

3 Acknowledgement

This work was sponsored by King Abdullah University of Science and Technology (KAUST) and used the resources of the KAUST Supercomputing Laboratory (KSL).

References

[1] Y. B. Zeldovich, Regime classification of an exothermic reaction with nonuniform initial conditions, Combust. Flame 39 (1980) 211–214.

[2] D. Bradley, C. Morley, X. J. Gu, D. R. Emerson, Amplified pressure waves during autoignition: Relevance to CAI engines, SAE Technical Paper (2002) 2002–01–2868.

[3] X. Gu, D. Emerson, D. Bradley, Modes of reaction front propagation from hot spots, Combust. Flame 133 (2003) 63–74.

[4] P. Dai, Z. Chen, S. Chen, Y. Ju, Numerical experiments on reaction front propagation in n-heptane/air mixture with temperature gradient, Proc. Combust. Inst. 35 (2015) 3045–3052.

[5] H. Yu, Z. Chen, End-gas autoignition and detonation development in a closed chamber, Combust. Flame 162 (2015) 4102–4111.

[6] P. Dai, C. Qi, Z. Chen, Effects of initial temperature on autoignition and detonation development in dimethyl ether/air mixtures with temperature gradient, Proc. Combust. Inst. 36 (2017) 3643–3650.

[7] P. Dai, Z. Chen, Effects of NOx addition on autoignition and detonation development in DME/air under engine-relevant conditions, Proc. Combust. Inst. 37 (2019) 4813–4820.

[8] H. Terashima, A. Matsugi, M. Koshi, Origin and reactivity of hot-spots in end-gas autoignition with effects of negative temperature coefficients: Relevance to pressure wave developments, Combust. Flame 184 (2017) 324–334.

[9] J. Pan, H. Wei, G. Shu, Z. Chen, P. Zhao, The role of low temperature chemistry in combustion mode development under elevated pressures, Combust. Flame 174 (2016) 179–193.

[10] J. Pan, H. Wei, G. Shu, R. Chen, Effect of pressure wave disturbance on auto-ignition mode transition and knocking intensity under enclosed conditions, Combust. Flame 185 (2017) 63–74.

[11] M. B. Luong, H. G. Im, Effects of low-temperature chemistry on detonation under engine-relevant conditions, Proc. Combust. Inst. 39 (2023) https://doi.org/10.1016/j.proci.2022.11.008.

[12] M. B. Luong, H. G. Im, Prediction of the developing detonation in an NTC-fuel/air mixture with temperature inhomogeneities under engine conditions, Proc. Combust. Inst. 39 (2023) https://doi.org/10.1016/j.proci.2022.10.015.

[13] Y. Morii, A. K. Dubey, H. Nakamura, K. Maruta, Two-dimensional laboratory-scale DNS for knocking experiment using n-heptane at engine-like condition, Combust. Flame 223 (2021) 330–336.

[14] M. B. Luong, S. Desai, F. E. Hernández Pérez, R. Sankaran, B. Johansson, H. G. Im, A statistical analysis of developing knock intensity in a mixture with temperature inhomogeneities, Proc. Combust. Inst. 38 (2021) 5781–5789.

[15] M. B. Luong, S. Desai, F. E. Hernández Pérez, R. Sankaran, B. Johansson, H. G. Im, Effects of turbulence and temperature fluctuations on knock development in an ethanol/air mixture, Flow Turbul. Combust. 106 (2021) 575–595.

[16] M. B. Luong, H. G. Im, Direct numerical simulation of preignition and knock in engine conditions, in: Advances in Energy and Combustion, 2022, pp. 311–336.

[17] M. B. Luong, F. E. Hernández Pérez, H. G. Im, Prediction of ignition modes of NTC-fuel/air mixtures with temperature and concentration fluctuations, Combust. Flame 213 (2020) 382–393.

[18] M. Figueroa-Labastida, M. B. Luong, J. Badra, H. G. Im, A. Farooq, Experimental and computational studies of methanol and ethanol preignition behind reflected shock waves, Combust. Flame 234 (2021) 111621.

[19] M. B. Luong, H. G. Im, Prediction of ignition modes in shock tubes relevant to engine conditions, in: Engines and Fuels for Future Transport, Energy, Environment, and Sustainability, 2022, pp. 369–393.

[20] M. B. Luong, F. E. Hernández Pérez, A. Sow, H. G. Im, Prediction of ignition regimes in DME/air mixtures with temperature and concentration fluctuations, AIAA SciTech 2019 Forum (2019) https://doi.org/10.2514/6.2019–2241.

[21] J. Zhang, M. B. Luong, F. E. Hernández Pérez, D. Han, H. G. Im, Z. Huang, Exergy loss of dme/air mixtures and ethanol/air mixtures with temperature and concentration fluctuations under HCCI/SCCI conditions: A DNS study, Combust. Flame 226 (2021) 334–346.

[22] G. H. Yu, M. B. Luong, S. H. Chung, C. S. Yoo, Ignition characteristics of a temporally evolving n-heptane jet in an iso-octane/air stream under RCCI combustion-relevant conditions, Combust. Flame 208 (2019) 299–312.

[23] A. Bhagatwala, Z. Luo, H. Shen, J. A. Sutton, T. Lu, J. H. Chen, Numerical and experimental investigation of turbulent DME jet flames, Proc. Combust. Inst. 35 (2015) 1157–1166.

[24] N. Peters, B. Kerschgens, G. Paczko, Super-knock prediction using a refined theory of turbulence, SAE Int. J. Engines 6 (2013) 953–967.